Generalized Wannier functions: A comparison of molecular electric dipole polarizabilities

David D. O'Regan,[1,2,*] Mike C. Payne,[1] and Arash A. Mostofi[3]

[1]*Cavendish Laboratory, University of Cambridge, J. J. Thomson Avenue, Cambridge CB3 0HE, United Kingdom*

[2]*Theory and Simulation of Materials, École Polytechnique Fédérale de Lausanne, 1015 Lausanne, Switzerland*

[3]*The Thomas Young Centre and the Department of Materials, Imperial College London, London SW7 2AZ, United Kingdom*

(Received 20 March 2012; revised manuscript received 3 May 2012; published 14 May 2012)

Localized Wannier functions provide an efficient and intuitive means by which to compute dielectric properties from first principles. They are most commonly constructed in a post-processing step, following total-energy minimization. Nonorthogonal generalized Wannier functions (NGWFs) [Skylaris *et al.*, Phys. Rev. B **66**, 035119 (2002); Skylaris *et al.*, J. Chem. Phys. **122**, 084119 (2005)] may also be optimized *in situ*, in the process of solving for the ground-state density. We explore the relationship between NGWFs and orthonormal, maximally localized Wannier functions (MLWFs) [Marzari and Vanderbilt, Phys. Rev. B **56**, 12847 (1997); Souza, Marzari, and Vanderbilt, *ibid.* **65**, 035109 (2001)], demonstrating that NGWFs may be used to compute electric dipole polarizabilities efficiently, with no necessity for post-processing optimization, and with an accuracy comparable to MLWFs.

DOI: 10.1103/PhysRevB.85.193101 PACS number(s): 71.15.Ap, 78.20.Bh, 31.15.ap, 31.15.E−

In this Brief Report, we explore the equivalence between nonorthogonal generalized Wannier functions (NGWFs),[1] generated using linear-scaling Kohn-Sham density functional theory (DFT),[3] and their orthonormal counterparts, particularly maximally localized Wannier functions (MLWFs),[2] both recently reviewed in Ref. 4. We demonstrate the comparable, high accuracy of the two formalisms for dielectric response, laying the foundation for large-scale calculation of optical properties.

We begin with the single-particle density-matrix defined for a given set of Bloch orbitals $|\psi_{n\mathbf{k}}\rangle$, where n indexes occupied bands, $\mathbf{k}$ is the crystal wave-vector, and we suppress the spin index for notational clarity, by

$$\hat{\rho} = \sum_n \int_{1\mathrm{BZ}} d\mathbf{k} |\psi_{n\mathbf{k}}\rangle f_{n\mathbf{k}} \langle\psi_{n\mathbf{k}}|. \tag{1}$$

Here, 1BZ is the first Brillouin zone corresponding to the periodic unit cell of volume V_{cell}. A reformulation of such Bloch states suitable for the study of spatially localized properties was proposed by Wannier,[5] whose eponymously named functions are defined for a unit cell at the lattice vector $\mathbf{R}$, by

$$|w_{n\mathbf{R}}\rangle = \sqrt{\frac{V_{\mathrm{cell}}}{(2\pi)^3}} \int_{1\mathrm{BZ}} d\mathbf{k}\, e^{-i\mathbf{k}\cdot\mathbf{R}} |\psi_{n\mathbf{k}}\rangle. \tag{2}$$

The orthonormality of Bloch orbitals is preserved,

$$\langle w_{n\mathbf{R}} | w_{m\mathbf{R}'}\rangle = \delta_{nm}\delta_{\mathbf{R}\mathbf{R}'}, \tag{3}$$

and we may choose the gauge freely, so that any prior unitary transformation among the orbitals, $|\tilde{\psi}_{n\mathbf{k}}\rangle = \sum_m |\psi_{m\mathbf{k}}\rangle U_{mn\mathbf{k}}$, may also give rise to a valid set of generalized Wannier functions, via Eq. (2). Unoccupied states may be included in the wannierization, while maintaining the same occupied density, by appropriately transforming the occupancy of the orbitals $f_{n\mathbf{k}}$, to give $\tilde{f}_{nm\mathbf{k}} = \sum_p U^\dagger_{np\mathbf{k}} f_{p\mathbf{k}} U_{pm\mathbf{k}}$. The density-matrix may be readily expressed in terms of Wannier functions, in the separable form proposed in Ref. 6, and given by

$$\hat{\rho} = \sum_{\mathbf{R}\mathbf{R}'} |w_{n\mathbf{R}}\rangle k_{nm\mathbf{R}'-\mathbf{R}} \langle w_{m\mathbf{R}'}|, \qquad \text{where} \tag{4a}$$

$$k_{nm\mathbf{R}} = \frac{V_{\mathrm{cell}}}{(2\pi)^3} \int_{1\mathrm{BZ}} d\mathbf{k}\, e^{-i\mathbf{k}\cdot\mathbf{R}} \tilde{f}_{nm\mathbf{k}} \tag{4b}$$

is commonly known as the *density kernel*.

The extension of this formalism to nonorthogonal generalized Wannier functions (NGWFs) is both of practical interest and utility. Orthonormality and spatial localization are generally competing requirements,[7] hence nonorthogonal orbitals may form a more efficient basis in which to expand short-ranged operators and, as a result, they are used extensively in linear-scaling DFT approaches. We may express these NGWFs, $|\phi_{\alpha\mathbf{R}}\rangle$, simply in terms of the generalization of the transformation matrices $U_{\mathbf{k}}$ to possible non-unitarity matrices $M_{\mathbf{k}}$; that is, $M_{n\alpha\mathbf{k}} = \langle\psi_{n\mathbf{k}}|\tilde{\psi}_{\alpha\mathbf{k}}\rangle$, whereafter $\tilde{f}_{\alpha\beta\mathbf{k}} = \sum_n M^\dagger_{\alpha n\mathbf{k}} f_{n\mathbf{k}} M_{n\beta\mathbf{k}}$. We use Latin and Greek letters to index orthonormal and nonorthogonal sets, respectively, and implicitly sum over repeated index pairs.

In the nonorthogonal case, the density-matrix may be expanded in separable form via the tensor contraction

$$\hat{\rho} = \sum_{\mathbf{R}\mathbf{R}'} |\phi_{\alpha\mathbf{R}}\rangle K^{\alpha\beta}_{\mathbf{R}'-\mathbf{R}} \langle\phi_{\beta\mathbf{R}'}|, \qquad \text{where} \tag{5a}$$

$$K^{\alpha\beta}_{\mathbf{R}} = \frac{V_{\mathrm{cell}}}{(2\pi)^3} \int_{1\mathrm{BZ}} d\mathbf{k}\, e^{-i\mathbf{k}\cdot\mathbf{R}} S^{\alpha\gamma} \tilde{f}_{\gamma\delta\mathbf{k}} S^{\delta\beta}, \tag{5b}$$

and the price to be paid for nonorthogonality is a nontrivial metric tensor given by $S_{\alpha\beta} = \langle\phi_{\alpha\mathbf{R}}|\phi_{\beta\mathbf{R}'}\rangle\delta_{\mathbf{R}\mathbf{R}'}$, which defines the interrelationship between covariant vectors, $|\phi_{\alpha\mathbf{R}}\rangle = |\phi^\beta_{\mathbf{R}}\rangle S_{\beta\alpha}$, and contravariant vectors (NGWF duals) $|\phi^\alpha_{\mathbf{R}}\rangle = |\phi_{\beta\mathbf{R}}\rangle S^{\beta\alpha}$. The contravariant metric $S^{\alpha\beta}$ in Eq. (5b) is defined such that $S_{\alpha\gamma}S^{\gamma\beta} \equiv \delta_\alpha{}^\beta$, and is also independent of the lattice vector. Orthonormality is thus replaced by the general tensor expression

$$\langle\phi_{\alpha\mathbf{R}}|\phi_{\gamma\mathbf{R}'}\rangle S^{\gamma\beta} = S_{\alpha\gamma}\langle\phi^\gamma_{\mathbf{R}}|\phi^\beta_{\mathbf{R}'}\rangle = \delta_\alpha{}^\beta\delta_{\mathbf{R}\mathbf{R}'}. \tag{6}$$

Numerous optimization procedures have been developed for *ab initio* Wannier functions. A widespread approach involves their construction in a post-processing step, computing the $U_{nm\mathbf{k}}$ or $M_{n\alpha\mathbf{k}}$ matrices, and then the generalized occupancies $\tilde{f}_{\mathbf{k}}$, *following* the computation of the delocalized orbitals. However, it has been recognized, and utilized in the context of large-scale calculations for some time,[8] that localized Wannier functions may also be optimized directly *in situ*; that is, during the process of solving for the electronic structure. In the latter, the basis expansion of the functions $\{\phi_{\alpha\mathbf{R}}(\mathbf{r})\}$ and the corresponding density kernel $K_{\mathbf{R}}^{\alpha\beta}$ must be optimized together, reconstructing the delocalized orbitals afterwards only if necessary.

A variety of plausible criteria may also be employed for Wannier function optimization in either case, such as energy downfolding[9] or maximal Coulomb repulsion,[10] or, as used in this work, total-energy minimization or spatial localization. Depending on their definition, these criteria may or may not uniquely define the Wannier functions, in that they may admit some residual gauge freedom. A particularly efficacious measure for localization is the second central moment which, for a set of Wannier functions $\{|w_{n\mathbf{R}}\rangle\}$ takes the form of the *spread* functional,

$$\Omega = \sum_{n} [\langle w_{n\mathbf{0}}|r^2|w_{n\mathbf{0}}\rangle - \langle w_{n\mathbf{0}}|\mathbf{r}|w_{n\mathbf{0}}\rangle^2], \tag{7}$$

where the generalization to the nonorthogonal case does not yield straightforward physical interpretation. MLWFs[2] are those orthonormal Wannier functions generated by unitary transformations $U_{nm\mathbf{k}}$ that minimize Ω, for a fixed set of orbitals. MLWFs are usually computed in a post-processing procedure, using an implementation such as WANNIER90,[11] and have been widely adopted as an accurate minimal basis with which to compute numerous ground-state and excited-state properties, as well as to augment DFT with many-body interactions.[4] MLWFs have been used to great effect, moreover, in the context of molecular dynamics, particularly interesting examples including the calculation of the dielectric permittivity and dipolar correlation of liquid water,[12] as well as its dynamical charge and dipole tensors.[13]

NGWFs, unlike their orthonormal counterparts, are more commonly optimized *in situ*, as a by-product of total-energy minimization with respect to the density-matrix, for example, in the ONETEP linear-scaling DFT code.[1,14] In the latter, NGWFs are expanded in a fixed underlying basis of periodic cardinal sine functions (also known as *psinc*[15] or bandwidth-limited δ-functions), whose spatial finesse is determined by a single variational parameter, the kinetic energy cutoff of the equivalent plane-wave basis. The NGWFs are then those functions, when traced with their corresponding optimized density kernel, which reproduce the ground-state density-matrix, whence the ground-state energy

$$\begin{aligned} E_0 &= \min_{n} E[n] = \min_{\hat{\rho}} E[\hat{\rho}]_{\hat{\rho}=\hat{\rho}^2} \\ &= \min_{\mathbf{K},\{\phi\}} E[\mathbf{K},\{\phi\}]_{\mathbf{K}=\mathbf{KSK}}. \end{aligned} \tag{8}$$

In practice, in order to extremize the total-energy with respect to idempotent density-matrices, two nested conjugate-gradient variational minimization procedures are performed. In the inner loop, the energy is minimized with respect to the elements of the density kernel, for a fixed NGWF expansion, and in the outer, the density kernel is kept fixed while the total-energy is minimized with respect to the NGWF psinc expansion. A number of similar methods have been proposed in which equations of motion generate optimized nonorthogonal functions.[8]

An intuitive interpretation of Wannier functions is furnished via the modern theory of polarization,[16] in that changes in their centers $\langle\mathbf{r}\rangle_{nm} = \langle w_{n\mathbf{0}}|\mathbf{r}|w_{m\mathbf{0}}\rangle$ exactly reproduce, and thus may be used to efficiently calculate, changes in the polarization of insulating systems. The change in electronic polarization $\delta\mathbf{P}$, subject to a gap-preserving perturbation, may be expressed as

$$\delta\mathbf{P} = -\frac{2e}{V_{\text{cell}}} \sum_{n}^{N} \delta\langle\mathbf{r}\rangle_{nn} \quad (\text{if } \tilde{f}_{nm} = \delta_{nm}, n \leqslant N), \tag{9a}$$

$$= -\frac{2e}{V_{\text{cell}}} \left[\delta K_{\mathbf{0}}^{\alpha\beta} \langle\mathbf{r}\rangle_{\beta\alpha} + K_{\mathbf{0}}^{\alpha\beta} \delta\langle\mathbf{r}\rangle_{\beta\alpha}\right], \tag{9b}$$

where the $\mathbf{k}$-independence of the occupancies (also spin degenerate) implies that it is sufficient to consider only the $\mathbf{R} = \mathbf{0}$ term. Here, respectively, we have provided the orthonormal case for N occupied bands, and the more general, nonorthogonal case.

It has been shown that close-to-orthonormal Wannier functions generated by means of direct minimization of an appropriately constructed functional may be used to efficiently compute dielectric properties.[17] It is of importance, particularly for linear-scaling methods, to generalize this result and verify that *in situ* optimized NGWFs can reproduce electronic response properties with the same reliability as that of the well-documented MLWFs, as NGWFs are increasingly being used in large-scale methods for spectral partitioning and dielectric properties, particularly in molecular systems.[18] The simplest such response property is perhaps the high-frequency (termed "clamped-ion" or "static") linear dipole polarizability tensor

$$\alpha_{ij} = \lim_{\omega\to\infty} \alpha_{ij}(\omega) = \left.\frac{\partial P_i}{\partial \mathcal{E}_j}\right|_{\delta\mathbf{R}_{\text{ion}}=0}, \tag{10}$$

where $\mathcal{E}$ is an applied electric field within the dipole approximation. This polarizability is somewhat different from that which is most frequently probed experimentally, namely, the static or visual frequency regimes, and neglects the response of the ionic positions.

Two different Kohn-Sham DFT packages were used in order to compute polarizabilities within the NGWF and MLWF formalisms; respectively, the ONETEP linear-scaling code[1,14] and a combination of a plane-wave pseudopotential package[29] and the WANNIER90 (Ref. 11) code. An example of each type of function is depicted in Fig. 1. A set of well-isolated, closed-shell molecules were selected, so that a sawtooth-potential representation of the electric field could be used, with the potential boundary maximally distant from the molecules, up to a maximum field value of $\pm 8.0 \times 10^{-5}$ Ha $e^{-1}a_0^{-1}$, in intervals of 2.0×10^{-5} Ha $e^{-1}a_0^{-1}$, for all systems. The response remained well within the linear regime at these field values, which lay well below the threshold for Zener breakdown. The rates of change in polarization were calculated using

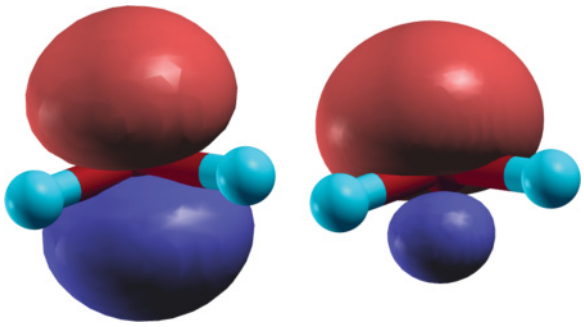

FIG. 1. (Color online) Wannier functions, NGWF (left) and MLWF (right), of predominantly oxygen p_{z^2} (highest occupied, $1b_1$) character in H_2O at zero applied field, with isosurfaces at one-sixth of their respective maxima. Both types retain some residual arbitrariness following optimization.

linear regression of finite-difference data. Identical norm-conserving pseudopotentials[30] were used in both cases; having been generated in the required formats, the Perdew-Burke-Ernzerhof (PBE) exchange-correlation approximation[28] and the same run-time parameters and analysis were used for both codes so far as possible. Zero-field ground-state geometries were optimized using ONETEP in cubic simulation cells of side length $40a_0$ ($50a_0$ in the case of naphthalene $C_{10}H_8$). The density and potential were fully reset to those of atomic superpositions upon each incrementation of the field. An equivalent plane-wave cutoff of 1000 eV, Γ-point Brillouin zone sampling, no density-kernel truncation, and NGWFs with a $10a_0$ radius cutoff were used.

In the case of nonaxially symmetric molecules, random initial guesses for the MLWFs were regenerated at each incrementation of the electric field. For axially symmetric molecules such as CO, CO_2, and N_2, however, the maximal localization condition does not uniquely define the MLWF centers under rotations about the axis, as discussed in Ref. 31. While the sum of centers, and hence the transverse response, should be well defined, in practice this unbroken symmetry results in excessively noisy linear-response data. It was found, however, that reinitializing the MLWFs to s orbitals at each field value, with centers coinciding with a set of zero-field MLWFs, proved sufficiently robust to obtain excellent linear fitting. No such measures were necessary in the case of ONETEP NGWFs, due to an effective symmetry breaking introduced by the underlying real-space psinc grid.

The isotropic and anisotropic parts of the polarizability tensor α are defined, respectively, as

$$\bar{\alpha} = \tfrac{1}{3}\mathrm{tr}[\alpha], \qquad \kappa = \sqrt{\tfrac{3}{2}\mathrm{tr}[\alpha^2] - \tfrac{1}{2}(\mathrm{tr}[\alpha])^2}, \tag{11}$$

our computed values of which using NGWFs and MLWFs are shown in Table I. The quadratic mean fractional discrepancy between the isotropic parts was 8.0×10^{-3}, while the discrepancy was greater for the anisotropic parts, at 4.1×10^{-2}. As judged by the arithmetic mean fractional discrepancies (given henceforth in parentheses), the NGWFs tended to provide slightly larger isotropic parts

TABLE I. Isotropic ($\bar{\alpha}$) and anisotropic (κ) polarizabilities ($e^2a_0^2\,\mathrm{Ha}^{-1}$) from DFT using nonorthogonal (NGWF) and orthonormal (MLWF) Wannier functions. Previous Gaussian-basis calculations (Ref. 28) and experimental values are included.

$\bar{\alpha}$	NGWF	MLWF	Gaussian	Experiment
H_2O	10.58	10.47	10.76,[a] 7.4[b]	9.64,[d] 9.79[f]
NH_3	15.28	15.24	15.63,[a] 12.1[b]	14.56,[d] 18.9[e]
CH_4	17.70	17.49	17.74,[a] 14.8[b]	17.27,[d] 17.5[e,f]
C_2H_4	28.50	28.39	28.77,[a]. 25.6[b]	27.70,[d] 28.69[f]
CO	13.64	13.53	13.73,[a] 12.1[b]	13.09,[d] 12.8,[e] 13.16[f]
CO_2	18.00	17.85	18.06,[a] 14.8[b]	17.51,[d] 19.6,[e,f] 17.48[f]
N_2	11.99	11.87	12.31,[a] 10.8[b]	11.74,[d,f] 11.5[e]
$C_{10}H_8$	122.8	123.0	121.76[c]	117.4,[g,h] 118.9[i]
κ	NGWF	MLWF	Gaussian	Experiment
H_2O	0.16	0.14	0.14[a]	0.67[d]
NH_3	2.45	2.64	2.70[a]	1.94[d]
C_2H_4	12.18	12.03	11.94[a]	11.4[d]
CO	3.53	3.54	3.55[a]	3.57[d]
CO_2	13.88	13.96	13.70[a]	13.83,[d] 13.70[f]
N_2	4.50	4.55	4.83[a]	4.59,[d] 4.45[f]
$C_{10}H_8$	96.1	94.8	94.13[c]	86.9,[g] 79.0,[h] 63.6[i]

[a]Static polarizability in a d-aug-cpVTZ basis (Ref. 19).
[b]Static PBE polarizability in 6-311++G(d,p) basis at B3LYP/6-311G** optimized geometries (Ref. 20).
[c]Static polarizability in Sadlej pVTZ basis (Ref. 21).
[d]Compiled in Ref. 19, based on analysis of anisotropy data (Ref. 22).
[e]CRC Handbook (Ref. 23).
[f]Extrapolated Rayleigh scattering (Ref. 24).
[g]Anisotropic refraction (Ref. 25).
[h]Laser Stark spectroscopy (Refs. 25 and 26).
[i]Optical measurements at 632.8 nm in solution (Ref. 27).

TABLE II. Probable fractional errors in molecular electric polarizabilities computed using NGWFs and MLWFs.

$\Delta\bar{\alpha}/\bar{\alpha}$	NGWF	MLWF	$\Delta\kappa/\kappa$	NGWF	MLWF
H_2O	1×10^{-4}	8×10^{-5}	NH_3	8×10^{-3}	8×10^{-3}
NH_3	3×10^{-3}	5×10^{-5}	NH_3	4×10^{-2}	5×10^{-4}
CH_4	1×10^{-4}	5×10^{-5}	CH_4	–	–
C_2H_4	3×10^{-5}	3×10^{-5}	C_2H_4	2×10^{-4}	2×10^{-4}
CO	2×10^{-4}	3×10^{-4}	CO	2×10^{-3}	2×10^{-3}
CO_2	2×10^{-5}	2×10^{-4}	CO_2	5×10^{-5}	4×10^{-4}
N_2	6×10^{-6}	3×10^{-4}	N_2	5×10^{-5}	2×10^{-3}
$C_{10}H_8$	4×10^{-4}	4×10^{-4}	$C_{10}H_8$	1×10^{-3}	1×10^{-3}

(by 6.6×10^{-3}), and also anisotropic parts (by 1.3×10^{-3}), than the MLWFs. Perhaps serendipitously, the NGWF values lay closer than the MLWF results, for the isotropic parts, in all cases, to the previous DFT (PBE) calculations of Ref. 19, computed using a sophisticated time-dependent coupled-perturbed method with a triple-ζ Gaussian basis set; the quadratic (arithmetic) mean discrepancies with respect to these previous results were 1.5×10^{-2} (1.3×10^{-2}) and 2.2×10^{-2} (2.0×10^{-2}), respectively. The trend was reversed for anisotropies.

Polarizabilities calculated using the related Wannier function varieties agree rather well in spite of the significant technical dissimilarities between the *ab initio* packages generating them, and there are a number of possible origins for the small discrepancies observed. First considering the NGWF and MLWF values, both based on the plane-wave formalism and using the same ionic geometry, the NGWF method is the more approximate in that it spatially truncates the Wannier functions and the kinetic-energy operator. Moreover, these methods differ in their handling of pseudopotentials and, substantially, in their energy-minimization algorithms. With respect to the previous Gaussian-basis results of Ref. 19, the possible origins for discrepancy are manifold, most notably, the ionic geometries employed differ and the latter method treats the core electrons explicitly.

The probable errors (arising from the linear fit to the data) in the isotropic and anisotropic polarizabilities, denoted $\Delta\bar{\alpha}$ and $\Delta\kappa$, respectively, and given by

$$\Delta\bar{\alpha} = \sqrt{\sum_{ij}\left(\frac{\partial\bar{\alpha}}{\partial\alpha_{ij}}\Delta\alpha_{ij}\right)^2} = \frac{1}{3}\sqrt{\sum_{i}(\Delta\alpha_{ii})^2}, \quad (12a)$$

$$\Delta\kappa = \kappa^{-1}\sqrt{\sum_{ij}\left[\left(\frac{3\alpha_{ji}}{2} - \sum_{k}\alpha_{kk}\frac{\delta_{ji}}{2}\right)\Delta\alpha_{ij}\right]^2}, \quad (12b)$$

were computed using the unbiased variance estimate $(\Delta\alpha_{ij})^2$ on each polarizability component α_{ij}, and are shown in Table II. The noise in the data for NGWFs is somewhat more system dependent, as the NGWF truncation depends on the ionic geometry, and higher than in the MLWF case for most of the molecules studied. The quadratic (arithmetic) mean of the ratio of the estimated error in the isotropic polarizability $\bar{\alpha}$ to its value was estimated at 1×10^{-3} (4×10^{-4}) for NGWFs and 2×10^{-4} (2×10^{-4}) for MLWFs. Correspondingly, for the anisotropic part $\Delta\alpha$, we estimated these ratios to be, respectively, 1×10^{-2} (7×10^{-3}) and 3×10^{-3} (2×10^{-3}). Nonetheless, the probable errors in the linear fits to the polarizability data were extremely small using both methods, and inconsequential with respect to the expected errors in the approximate functional.

In conclusion, we have shown that nonorthogonal Wannier functions optimized *in situ* may be used to compute molecular polarizabilities with an accuracy comparable to MLWFs post-processed from plane-wave DFT. This result is promising for the computation of numerous dielectric properties, and the full application of linear-scaling Wannier function analysis to large systems. A promising avenue for future work is the generalization of a method for the dielectric response in extended systems, such as that described in Ref. 32 and applied to solids in Ref. 17, to the linear-scaling NGWF formalism.

We are grateful to John Biggins and Danny Cole for helpful discussions, and to Mark Robinson and Peter Haynes for provision of software. D.D.O'R acknowledges the support of EPSRC and the National University of Ireland. M.C.P. acknowledges EPSRC support (Grants No. EP/G055904/1 and No. EP/F032773/1). A.A.M. acknowledges the support of EPSRC (EP/G05567X/1) and RCUK.

*david.oregan@epfl.ch

[1] C.-K. Skylaris, A. A. Mostofi, P. D. Haynes, O. Diéguez, and M. C. Payne, Phys. Rev. B **66**, 035119 (2002); C.-K. Skylaris, P. D. Haynes, A. A. Mostofi, and M. C. Payne, J. Chem. Phys. **122**, 084119 (2005).

[2] N. Marzari and D. Vanderbilt, Phys. Rev. B **56**, 12847 (1997); I. Souza, N. Marzari, and D. Vanderbilt, *ibid.* **65**, 035109 (2001).

[3] P. Hohenberg and W. Kohn, Phys. Rev. **136**, B864 (1964); W. Kohn and L. J. Sham, *ibid.* **140**, A1133 (1965).

[4] N. Marzari, A. A. Mostofi, J. R. Yates, I. Souza, and D. Vanderbilt, Rev. Mod. Phys. (in press), e-print arXiv:1112.5411.

[5] G. H. Wannier, Phys. Rev. **52**, 191 (1937).

[6] R. McWeeny, Rev. Mod. Phys. **32**, 335 (1960).

[7] P. W. Anderson, Phys. Rev. Lett. **21**, 13 (1968).

[8] E. Hernández and M. J. Gillan, Phys. Rev. B **51**, 10157 (1995); D. R. Bowler, T. Miyazaki, and M. J. Gillan, J. Phys.: Condens. Matter **14**, 2781 (2002); F. Mauri, G. Galli, and R. Car, Phys. Rev. B **47**, 9973 (1993); F. Mauri and G. Galli, *ibid.* **50**, 4316 (1994); P. Ordejón, D. A. Drabold, R. M. Martin, and M. P. Grumbach, *ibid.* **51**, 1456 (1995); T. Ozaki, *ibid.* **67**, 155108 (2003); S. Liu, J. M. Pérez-Jordá, and W. Yang, J. Chem. Phys. **112**, 1634 (2000).

[9] A. Yamasaki, M. Feldbacher, Y.-F. Yang, O. K. Andersen, and K. Held, Phys. Rev. Lett. **96**, 166401 (2006).

[10] T. Miyake and F. Aryasetiawan, Phys. Rev. B **77**, 085122 (2008).

[11] A. A. Mostofi, J. R. Yates, Y.-S. Lee, I. Souza, D. Vanderbilt, and N. Marzari, Comput. Phys. Commun. **178**, 685 (2008).

[12]M. Sharma, R. Resta, and R. Car, Phys. Rev. Lett. **98**, 247401 (2007).
[13]A. Pasquarello and R. Resta, Phys. Rev. B **68**, 174302 (2003).
[14]N. Hine, P. Haynes, A. Mostofi, C.-K. Skylaris, and M. Payne, Comput. Phys. Commun. **180**, 1041 (2009).
[15]A. A. Mostofi, P. D. Haynes, C.-K. Skylaris, and M. C. Payne, J. Chem. Phys. **119**, 8842 (2003).
[16]R. D. King-Smith and D. Vanderbilt, Phys. Rev. B **47**, 1651 (1993); R. Resta, Rev. Mod. Phys. **66**, 899 (1994).
[17]P. Fernández, A. Dal Corso, A. Baldereschi, and F. Mauri, Phys. Rev. B **55**, R1909 (1997); P. Fernández, A. Dal Corso, and A. Baldereschi, *ibid*. **58**, 7480R (1998).
[18]L. E. Ratcliff, N. D. M. Hine, and P. D. Haynes, Phys. Rev. B **84**, 165131 (2011); P. W. Avraam, N. D. M. Hine, P. Tangney, and P. D. Haynes, *ibid*. **85**, 115404 (2012); D. D. O'Regan, N. D. M. Hine, M. C. Payne, and A. A. Mostofi, *ibid*. **82**, 081102 (2010).
[19]C. van Caillie and R. D. Amos, Chem. Phys. Lett. **328**, 446 (2000).
[20]R. R. Zope, T. Baruah, M. R. Pederson, and B. I. Dunlap, Int. J. Quantum Chem. **108**, 307 (2008).
[21]J. R. Hammond, K. Kowalski, and W. A. deJong, J. Chem. Phys. **127**, 144105 (2007).
[22]T. N. Olney, N. M. Cann, G. Cooper, and C. E. Brion, Chem. Phys. **223**, 59 (1997); M. A. Spackman, J. Chem. Phys. **94**, 1288 (1991); J. Dougherty and M. A. Spackman, Mol. Phys. **82**, 193 (1994).
[23]*CRC Handbook*., 87th ed., edited by D. P. Lide (CRC Press, Boca Raton, FL, 2006).
[24]G. R. Alms, A. Burnham, and W. H. Flygare, J. Chem. Phys. **63**, 3321 (1975).
[25]H. F. Vuks, Opt. Spectrosc. **20**, 361 (1966).
[26]S. Heitz, D. Weidauer, B. Rosenow, and A. Hese, J. Chem. Phys. **96**, 976 (1992).
[27]R. L. Calvert and G. L. D. Ritchie, J. Chem. Soc., Faraday Trans. **2**, 1249 (1980).
[28]J. P. Perdew, K. Burke, and M. Ernzerhof, Phys. Rev. Lett. **77**, 3865 (1996).
[29]Quantum Espresso, http://www.quantum-espresso.org.
[30]Opium pseudopotentials, http://opium.sourceforge.net.
[31]L. Andrinopoulos, N. D. M. Hine, and A. A. Mostofi, J. Chem. Phys. **135**, 154105 (2011).
[32]R. W. Nunes and D. Vanderbilt, Phys. Rev. Lett. **73**, 712 (1994).